View Article Online
DOI: 10.1039/C9DT00751B

Dalton Transactions

RSCPublishing

COMMUNICATION

Temperature-assisted formation of reversible metallophilic Au-Ag interaction arrays

mCite this: DOI: 10.1039/xoxxoooooox

María Gil-Moles,[a] M. Concepción Gimeno,*[b] José M. López-de-Luzuriaga,*[a] Miguel Monge,[a] and M. Elena Olmos[a]

Received ooth December 2017,
Accepted ooth January 2017

DOI: 10.1039/xoxxoooooox

www.rsc.org/

A temperature controlled self-assembly process in solution of $[Ag(terpy)]_n^{n+}$ and $[Au(C_6F_5)_2]^-$ units has been performed. For this, the crystallisation of complex $[\{AuR_2\}Ag(terpy)]_n$ in the same experimental conditions, only changing the temperature, permits the synthesis of polymorphs $[\{Au(C_6F_5)_2\}_2Ag_2(terpy)_2]_n$ (**2a**) at 298 K and $[\{Au(C_6F_5)_2\}Ag(terpy)]_n$ (**2b**) at 280 K, respectively. The X-ray diffraction studies previously reported for **2a** revealed a polymeric structure with an unusual + + - - + + - - charge sequence, whereas for polymorph **2b** a more classical + - + - disposition has been obtained. The conversion of one polymorph into the other can be achieved by simple dissolution of one of them and recrystallisation at the corresponding temperature. The mechanism of formation of each polymorph is proposed in view of their ^{1}H NMR, ^{1}H-PGSE NMR and molar conductivity measurements.

Introduction

Molecular associations based on metallophilic interactions between closed-shell Au(I) and Ag(I) d^{10} ions represent an important class of self-assembled systems displaying unique photophysical properties related to these, in principle weak, metal-metal contacts.[1]

In several cases, this self-assembly appears assisted by supporting polydentate ligands such as bridging chalcogenides or thiolates combined with phosphinopyridines,[2,3] diphosphines with arylacetylenes,[4-6] or N-heterocyclic carbenes with pendant pyridine moieties,[7,8] among others. In such cases, the self-assembly through metallophilic Au(I)···Ag(I) interactions could be considered directed by the ligand architecture.

On the other hand, the spontaneous association between Au(I) and Ag(I) moieties leading to unsupported metallophilic interactions can be achieved through the use of an acid-base approach. This strategy has been previously studied by us[9-12] and others.[13,14] In our particular case, the synthetic approach consists in the reaction between basic bis(perhalophenyl)gold(I) precursors and acidic silver(I) salts in the presence of neutral donor ligands. This methodology has allowed us to synthesise different types of heterometallic arrangements. Among them, the most frequently observed are polymeric structures of aurophilically linked $-Au_2Ag_2-$ units, but polymeric chains displaying an alternated disposition of the metals (-Au-Ag-Au-Ag-) have also been obtained (see Scheme 1).

Nevertheless, we have recently observed that the ordering of the heterometallic interactions or, even, the influence of the molecular conformation in the Au-Ag metallophilic arrangements constitute versatile approaches for the presence and tuning of luminescent properties in solid state. Thus, for instance, we have taken advantage of a solvent-dependent structural isomerisation process leading to E- and Z-isomers of a discrete molecule with an unusual Ag-Au-Au-Ag arrangement.[15] In this case, the use of S-donor macrocyclic ligands bonded to Ag(I) precludes the formation of polymeric species or alternate intermetallic arrangements. The reversibility of the isomerisation process allows an interesting tuning of the luminescent properties of these complexes.

Additionaly, we have recently reported a purposeful strategy for the synthesis of heterometallic gold-silver arrangements displaying an unprecedented -Ag-Ag-Au-Au- disposition of the metallic fragments, disobeying Coulomb's rule. This metallic disposition, in contrast to the more expected alternated -Au-Ag-Au-Ag- one that fulfils Coulomb's rule, displays interesting emissive properties (see Scheme 1).[16]

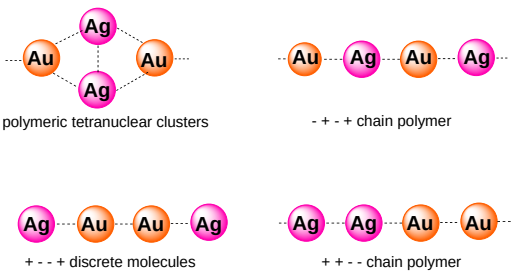

Scheme 1 Metallophilic Au-Ag arrangements found in solid state. Orange spheres labelled with Au represent anionic bis(perhalophenyl)aurate(I) units; pink spheres labelled with Ag represent Ag^+ centres bonded to neutral ligands.

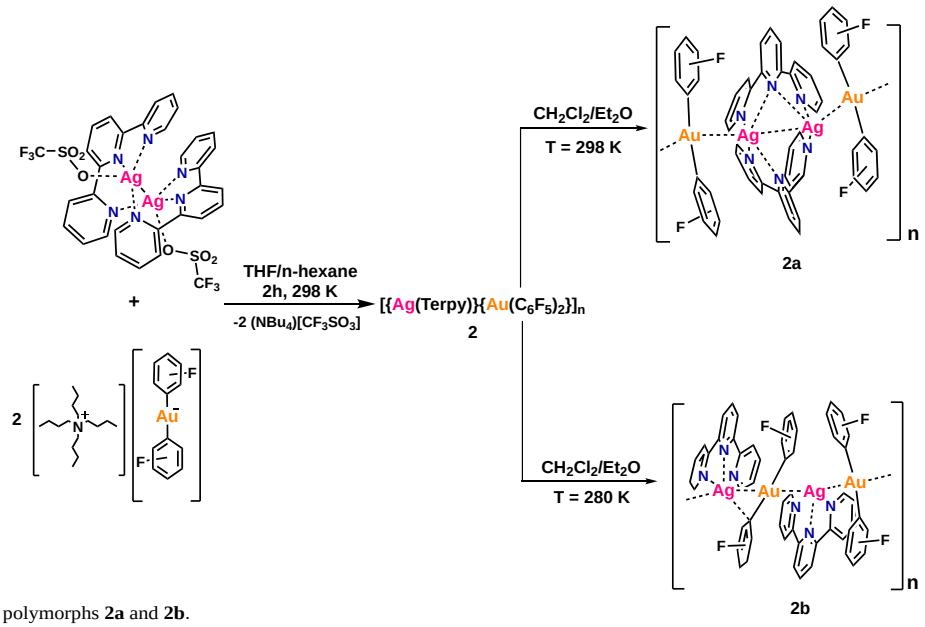

Scheme 2. Synthesis of polymorphs **2a** and **2b**.

In the latter study, the quest for such a different heterometallic disposition was preconceived by using the idea that a dinuclear $[Ag_2(terpy)_2]^{2+}$ unit keeping a supported Ag···Ag interaction would preclude the formation of a more common alternated Au-Ag-Au-Ag or Au_2Ag_2 cluster-like ones. In this study we explored the structural arrangements for the corresponding complexes built up with basic $[AuR_2]^-$ units (R = C_6F_5, $C_6Cl_2F_3$ and C_6Cl_5). From the obtained complexes, the ones with C_6F_5 and $C_6Cl_2F_3$ led to the formation of complexes of the type $[\{AuR_2\}_2Ag_2(terpy)_2]_n$ displaying this uncommon intermetallic disposition, but the one with C_6Cl_5 led to $[\{AuR_2\}Ag(terpy)]_n$, in which the alternated arrangement of metals was preferred, probably due to the higher steric hindrance of this perhalophenyl group.

In view of these results, we wondered about the possibility of controlling the formation of different metallophilic arrangements for a given complex. Thus, we thought that a step forward in this research field would be the possibility of performing a purposely and rational self-assembly of a given metallophilic arrangement and its further conversion into another one through the control of the environmental conditions. With this idea we would not only tune the structure-property relationship for a family of complexes displaying different Au-Ag arrangements, but we would also control the self-assembly process towards a certain intermetallic disposition and the possible change into another one, by the variation of its environment.

The ligand terpy is able to bind the silver centres in a chelate tridentate fashion, leading to $[Ag(terpy)]^+$ units, or as a bridging ligand, leading to $[Ag_2(terpy)_2]^{2+}$ ones. Following the previously commented idea of using the coordination abilities of terpy, we tried to exert a control of the self-assembly of this species with $[Au(C_6F_5)_2]^-$ units by the study of the effects of different environmental conditions in solution. For this purpose, we performed a systematic analysis of the influence of the crystallisation temperature or solvent, concentration in solution or nature of the halogens in the AuR_2^- basic units. We have used ^{1}H PGSE-NMR technique that permits the estimation of the molecular size of the Ag-terpy fragments in solution by the calculation of the hydrodynamic radii through the Stokes-Einstein equation.

Herein we report that, among all the parameters studied, the crystallisation temperature has a great influence on the control of the self-assembly of a heterometallic Au(I)-Ag(I) complex through metallophilic interactions. This control can be achieved through a delicate balance of the equilibrium in solution between the corresponding dinuclear $[Ag_2(terpy)_2]^{2+}$ units at room temperature (298 K) and the chelate tridentate coordination of terpy in $[Ag(terpy)]_n^{n+}$ units at lower temperature (280 K). Depending on the existence of these Ag-terpy species in solution, different metallophilic arrays can be achieved, leading to the uncommon -Ag-Ag-Au-Au- disposition at 25 ºC, and to the alternated -Au-Ag-Au-Ag- one at 7 ºC regardless of the solvent employed. In addition, the conversion between both metallophilic arrangements can be easily performed through simple dissolution of the corresponding polymorph, followed by crystallisation at the appropriate temperature.

Results and discussion

Synthesis and characterisation

We recently reported that the reaction of the dinuclear Ag(I) complex $[Ag_2(terpy)_2](CF_3SO_3)_2$ (**1**) with the basic gold(I) precursor $(NBu_4)[Au(C_6F_5)_2]$[16] in a 1:2 molar ratio in THF at room temperature led to the synthesis of a solid sample of complex **2** (Scheme **2**). Recrystallisation of **2** in CH_2Cl_2/Et_2O at

View Article Online
DOI: 10.1039/C9DT00751B
ARTICLE

room temperature gave rise to single crystals in which a -Ag-Ag-Au-Au- disposition of the metallic fragments was obtained as observed through X-ray diffraction studies. The XRD pattern of the solid sample precipitated in *n*-hexane from an evaporated THF solution matches the one obtained from the single crystals grown in CH_2Cl_2/Et_2O (see ESI), what confirms the same structural arrangement in both situations at room temperature and rules out a key role of the solvent in the formation of polymorph **2a**.

As we have commented in the Introduction section, the temperature is a key factor for controlling the aggregation process in solution (see below) and, therefore, the rearrangement of the atoms in the solid state crystal structure. Thus, when complex **2** was dissolved in CH_2Cl_2 or in THF at 280 K and crystallised by slow diffusion of Et_2O into this solution, a second polymorph, $[\{Au(C_6F_5)_2\}Ag(terpy)]_n$ (**2b**), was isolated, which displays an alternated polymeric -Au-Ag-Au-Ag- disposition of the metals (see Crystal Structures section). For this new polymorph **2b** the spectroscopic and analytical data are in agreement with the proposed stoichiometry.

Its IR spectrum displays the characteristic bands of the $[Au(C_6F_5)_2]^-$ units at 1502, 954, 781 cm^{-1}, as well as that corresponding to the ν(C=N) stretching vibration of the terpyridine rings at 1628-1568 cm^{-1} and ν(C-H) bending vibration at 1013-992 cm^{-1}. In these two regions, a characteristic pattern for each polymorph is in agreement with the different coordination modes of the terpy ligands to the silver centres. In the mass spectra MALDI-TOF(−) of solid samples of polymorphs **2a**[16] and **2b**, the base peak corresponding to the anion $[Au(C_6F_5)_2]^-$ is observed at *m/z* = 531. Their MALDI-TOF(+) mass spectra display a base peak corresponding to the cationic fragment $[Ag(terpy)]^+$ at *m/z* = 339.835, and second peak at *m/z* = 573, associated with the $[Ag(terpy)_2]^+$ fragment, confirming the presence of the silver counterpart. In all of them, the experimental isotopic distributions are in agreement with the calculated ones. In addition, in their mass spectra ESI(−), the experiments of exact mass for polymorphs **2a**[16] and **2b** show that the base peak corresponds to the anion $[Au(C_6F_5)_2]^-$ at *m/z* = 530.9506. In the ESI(+), the base peak assigned to the fragment $[\{Au(C_6F_5)_2\}Ag_2(terpy)_2]^+$ at *m/z* = 1210.9508 was observed for polymorphs **2a** and **2b**.

Crystal structures

The crystal structure of polymorph **2b** was unequivocally determined by X-ray diffraction studies from single crystals obtained by slow diffusion of diethyl ether into a solution of the complex in CH_2Cl_2 (**2b·CH₂Cl₂**) or THF (**2b·THF**) at 280K. Details of the data collection and refinement, as well as selected bond lengths and angles, are given in the ESI (Tables S3-S6).

Complex **2b** consist of a polymeric chain that runs parallel to the crystallographic *y* axis, and that is formed by $[Ag(terpy)]^+$ cations and $[Au(C_6F_5)_2]^-$ anions connected through intermetallic Au···Ag interactions and additional Ag···C_{ipso} contacts, showing a nearly linear -Ag-Au-Ag-Au- structural disposition (Figure 1). This arrangement fulfils Coulomb's rule, what precludes the formation of the dinuclear $[Ag_2(terpy)_2]^{2+}$ cations and, therefore, the Ag···Ag and Au···Au interactions observed for polymorph **2a**.[16] The Ag-Au distances of 2.7969(3) and 2.7747(3) Å in **2b·CH₂Cl₂** or of 2.8090(4) and 2.7882(4) Å in **2b·THF** are shorter than in polymorph **2a** (2.8979(5) Å) or in $[\{Au(C_6Cl_2F_3)_2\}_2Ag_2(terpy)_2]_n$, which is isostructural with **2a** (2.9956(4) and 2.9762(4) Å),[16] probably due to the alternation of positive and negative charges in **2b**, which avoids repulsions between the metallic fragments. In addition, the Au-Ag distances in **2b** are also shorter than those in $[\{Au(C_6Cl_5)_2\}Ag(terpy)]_n$ (2.8970(10) and 2.9070(10) Å),[16] where the same disposition of metals and non-bridging terpy ligands than in **2b** are observed, but that contains the bulkier pentachlorophenyl groups bonded to gold(I).

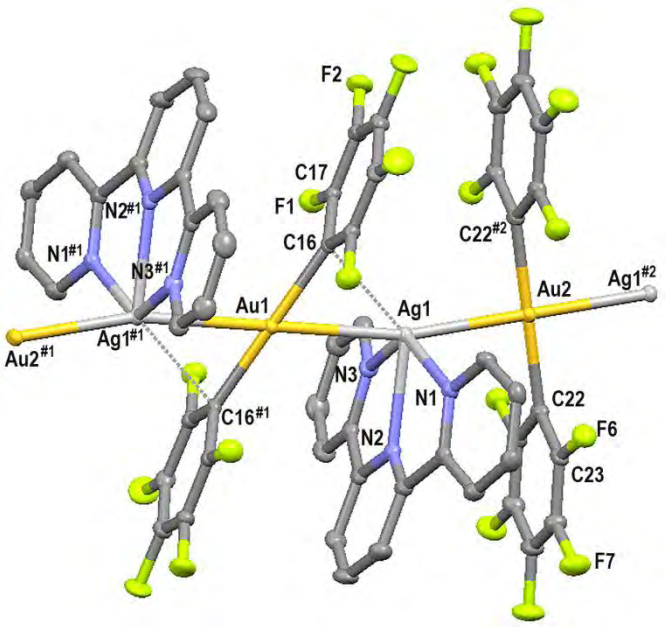

Fig. 1 Part of the polymeric crystal structure of **2b·CH₂Cl₂** with the labelling scheme for the atom positions. Ellipsoids are drawn at 30% level. Hydrogen atoms have been omitted for clarity. Symmetry transformations used to generate equivalent atoms: #1 -x+1,-y+1,-z #2 -x+1,-y+2,-z

The gold(I) centres in **2b** are linearly coordinated to two aryl groups, showing typical Au−C distances between 2.045(5) and 2.073(4) Å, while each silver atom is bonded to the three nitrogen centres of a terpy ligand with Ag-N bond distances varying from 2.390(4) and 2.427(4) Å in **2b·CH₂Cl₂** or from 2.395(2) and 2.512(4) Å in **2b·THF**. These distances compare well with those found in $[\{Au(C_6Cl_5)_2\}Ag(terpy)]_n$ (2.393(9)-2.404(9) Å),[16] and are longer than those described for the non-bridging N atoms of the terpy ligands in the crystal structure of **2a** (2.254(6)-2.285(5) Å) and $[\{Au(C_6Cl_2F_3)_2\}_2Ag_2(terpy)_2]_n$ (2.222(4) and 2.2612(4) Å).[16]

Additionally, each silver atom in **2b** maintains a Ag···C contact with the *ipso* carbon atom of a pentafluorophenyl ring, displaying Ag−C_{ipso} distances of 2.582(4) Å in **2b·CH₂Cl₂** or of 2.520(5) or 2.521(6) Å in **2b·THF**, which lie in the range of

Ag–C_{ipso} distances described for other Au/Ag related compounds (2.4396(6) to 2.687(6) Å).[9,10,12,17,18] Also, the presence of π-stacking interactions between C_6F_5 ligands and aromatic rings of the terpy ligand in **2b·CH$_2$Cl$_2$** (distances between centroids in the 3.837-3.860 Å range) and **2b·THF** (distance between centroids 3.074 Å) leads to attractive dispersive interactions similar to the ones previously described for pentafluorophenyl and phenyl substituents in Si-based complexes[19] or between pentafluorophenyl and pyridine ligands in heterometallic Au-Ag complexes.[20] Finally, the presence on C-H···F and C-H···Cl hydrogen bonds in **2b·CH$_2$Cl$_2$** gives rise to the formation of a 3D network (see ESI, Figure S5).

Photophysical studies

The absorptions of complexes in dichloromethane solutions are dominated by ligand transitions. The absorption spectrum of the silver complex $[Ag_2(terpy)_2](CF_3SO_3)_2$ (**1**) shows bands at 250-280 nm and 310 nm (see ESI), which are likely to arise from π → π * and n → π * transitions.[16] The UV-Vis spectra of polymorphs **2a** and **2b** in solution are identical both at 298 K and 280 K (see ESI) and we cannot observe the differences resulting from the different coordination modes of the terpy ligands that appear in the solid state spectra. In dichloromethane solution, the absorption bands for **2a** and **2b** are located at identical positions to those of complex **1**. The main difference between them is the intensity of absorption maxima of the heterometallic complexes in the range 250-280 nm, which is probably due to the overlapping with the π→π* absorptions assigned to the perhalogenated ligands.

In contrast to the absorption spectra in CH_2Cl_2 solutions, the absorption spectra of both polymorphs **2a** and **2b** in solid state show significant differences (see Figure **2**). These differences are attributable to the existence of different metallophilic interactions and coordination of the terpyridine ligands to the metal centres, since those due to the formers frequently appear in the less energetic zone of the spectra. Thus, complex **2a** shows a maximum absorption band at 230 nm and a shoulder near 300 nm with a tail up to ca. 420 nm. These bands are likely to be due to the π → π * and n → π * transitions in the perhalophenyl and in the terpyridine ligands, similarly to those appearing in the solution experiments. The tail is likely to contain transitions involving orbitals of the metal centres. Complex **2b** shows a different absorption spectrum consisting in a featureless broadband, whose maximum appears at ca. 350 nm extending to 420 nm. As in complexes **1** and **2a**, the higher energy part is likely to contain π→π* and n→π* absorptions located in the aromatic rings, while in the less energetic zone appear those absorptions in which the metal centres are involved.

The luminescence studies show that the emissive properties of these complexes are greatly influenced by the metallic ordering. Thus, while polymorph **2a** shows a luminescent emission at 550 nm (see ESI) assigned to a metal-metal (god-gold) to ligand (terpy) charge transfer transition (^{3}MMLCT) transition involving the interacting gold-gold centres,[16] polymorph **2b** does not display emissive properties. Obviously, the main differences between both polymorphs are the spatial arrangement of atoms, and, therefore, the different metallophilic interactions present. Thus, the presence or absence of Au···Au interactions in the complexes influences the existence of an emissive behaviour, as we observed in a previous work with related derivatives.[1]

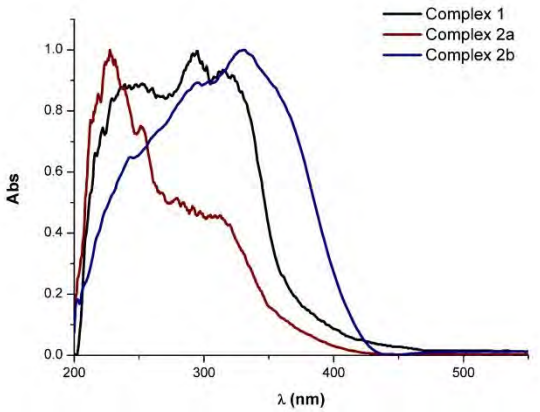

Fig. 2 Absorption spectra in solid state of complexes **1**, **2a** and **2b**.

^{1}H NMR and ^{1}H-PGSE-NMR Studies

Figure 3 depicts the ^{1}H NMR spectra of complex **2** in CD_2Cl_2 solution at different temperatures in the 298-193 K range. A first observation is that, upon cooling the sample, most of the signals associated to the protons of the terpyridine ligand gradually shift upfield together with some signal broadening.

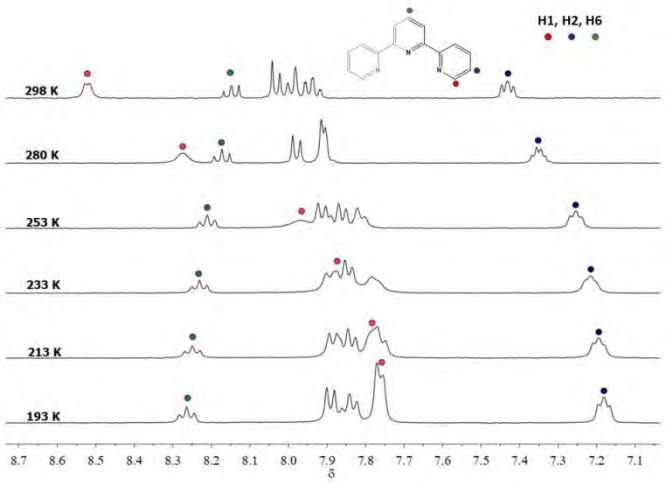

Fig. 3. ^{1}H-NMR spectra for complex **2** at different temperatures (298-193 K)

A similar behaviour of dipyridylbenzene ligand (CNC) was recently reported by Koshevoy et al for the cyclometalated $[Pt(CNC)(CNCH_3)]^+$ units in solution.[21] This upfield shift of signals was attributed to the formation of increasing length aggregates formed through the stacking of the individual Pt(II) moieties through π-π and/or Pt···Pt metallophilic interactions, in which the counterion did not seem to play an important role. Therefore, in our particular case, it seems that the nuclearity of

View Article Online
DOI: 10.1039/C9DT00751B
ARTICLE

the $[Ag(terpy)]_n^{n+}$ units increases as the temperature decreases, probably due to the formation of π-π and/or Ag···Ag interactions. At this regard, a previous study reported by Hannon et al,[22] showed that complexes of the type $[AgL]_n^{n+}$ (L = 4'-thiomethyl-2,2':6',2"-terpyridine) crystallised under certain conditions in form of polynuclear chains displaying Ag···Ag, π···π or Ag···π interactions that were kept in solution, as evidenced through ^{1}H NMR studies.

In addition, the largest shift upfield of the proton signals takes place at the highest temperature, what would suggest that the molecular changes in the first stages of the temperature lowering are even more drastic. This trend can be compared with the crystallographic results obtained for polymorphs **2a** (at 298 K) and **2b** (at 280 K), in which even the coordination of the terpyridine ligand changes from a bridging to a chelate mode.

Although the study of the ^{1}H NMR spectra of complex **2** relies interesting information that points to a different degree of association of $[Ag(terpy)]^+$ units with decreasing temperature, a plausible proposal for the drastic coordination mode change of the terpy ligands observed in the crystal structure characterisation of polymorphs **2a** and **2b** cannot be achieved with these data. In order to gain a deeper insight into this metallophilic array change, we performed variable-temperature ^{1}H pulsed-gradient spin-echo (PGSE) NMR experiments, which allow us to estimate the degree of aggregation of $[Ag(terpy)]^+$ units.

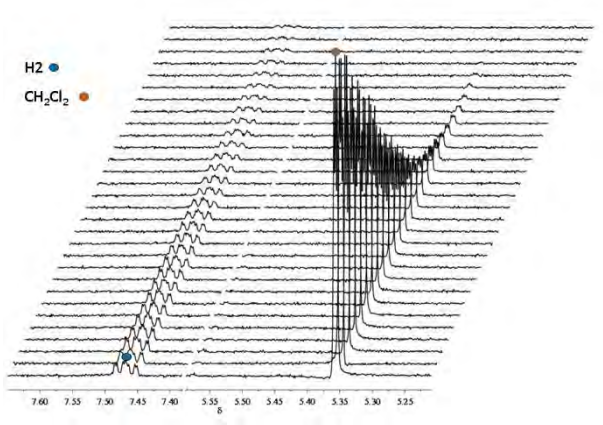

Fig. 4. ^{1}H-NMR spectra for complex **2** at different temperatures (298-193 K)

Thus, the ^{1}H-PGSE-NMR experiments provide the measurement of the translational self-diffusion coefficient D_t at each temperature. With this parameter and using the Stokes-Einstein equation, the hydrodynamic radius and, therefore, the hydrodynamic molecular volume can be evaluated (see ESI for details). ^{1}H-PGSE NMR experiments were carried out in CD_2Cl_2 at 298, 280, 253, 233 and 213 K for complex **2** at 1 mM concentration with the solvent signal as internal standard. The D_t coefficients were determined by ^{1}H PGSE NMR analysis of the H2 terpyridine proton, whose resonance appears between 7.47 ppm at 298 K and 7.20 ppm at 193 K (see Figure 4 and ESI).

From the obtained D_t coefficients we have estimated the hydrodynamic radii (r_H^2) and the hydrodynamic volume (V_H^2) of the molecular $[Ag(terpy)]_n^{n+}$ fragments in solution at each temperature (see Table 1). In order to estimate the degree of association of $[Ag(terpy)]^+$ fragments at each temperature we also performed the ^{1}H-PGSE NMR experiments for complex **1** in solution, which contains dinuclear $[Ag(terpy)]_2^{2+}$ fragments, as observed in its X-ray diffraction structure. Thus, the degree of association at each temperature was calculated by the V_H^2/V_H^1 ratio, where V_H^2 is the hydrodynamic volume for complex **2** in solution and V_H^1 is the hydrodynamic volume for complex **1** in solution.

Starting from the PGSE results at 298 K, the hydrodynamic volume for complex **1** was V_H^1 = 395.6 Å^3, whereas a fairly similar value was obtained for hydrodynamic volume for complex **2** of V_H^2 = 429.24 Å^3, leading to a V_H^2/V_H^1 ratio of 1.08, close to 1. This result already points to interesting conclusions. First, considering the calculated hydrodynamic volume ratio, we can conclude that complex **2** at 298 K in solution consists of dimeric $[Ag(terpy)]_2^{2+}$ units, since the degree of association is similar to that of complex **1** under similar conditions. In addition, we can also establish that the role played by the $[Au(C_6F_5)_2]^-$ moieties in solution for complex **2** is similar to the one played by the $CF_3SO_3^-$ anion, behaving as a mere anionic counterpart without metallophilic Au···Ag interactions at this temperature and concentration conditions.

However, if we analyse the ^{1}H-PGSE results at different temperatures, clear changes are observed. Table 1 displays the increase of the corresponding V_H^2/V_H^1 ratios with decreasing temperatures, which can be related to the formation of $[Ag(terpy)]_n^{n+}$ oligomers of increasing length, namely: 1.5 at 280 K, $[Ag(terpy)]_3^{3+}$; 1.98 at 253 K, $[Ag(terpy)]_{3.6}^{3.6+}$; 2.25 at 233 K, $[Ag(terpy)]_{4.5}^{4.5+}$; and 3.57 at 213, $[Ag(terpy)]_{6.5}^{6.5+}$. With these observations we propose that at temperatures below 298 K, a change in the $[Ag(terpy)]^+$ fragments disposition would take place, leading to the rupture of the double-bridged dinuclear Ag(I) metallacycle and to the formation of less-sterically hindered extended chain of Ag(I) centres with single terpyridine bridges, in agreement with the results previously reported by Hannon et al.[22] Thus, due to this drastic change in the structural arrangement of the $[Ag(terpy)]_n^{n+}$ fragments, different crystallisation processes would take place: at 298 K the formation of Au···Ag interactions, keeping the $[Ag(terpy)]_2^{2+}$ fragment, would occur, and, therefore, the polymeric -Au-Ag-Ag-Au- arrangement would appear in the solid state; while at 280 K the aurate(I) units would form $[Ag(terpy)]_n^{n+}$ (n ≥ 3) oligomers, leading to the alternated polymeric -Au-Ag-Au-Ag- pattern during the crystallisation process (see scheme 3). In both cases, a delicate balance between strong ionic plus dispersive Au···Ag interactions and dispersive π-stacking (between terpy ligands or terpy-C_6F_5 aromatic rings) or Ag···C_{ipso} ones would allow the formation of both polymorphs in solid state at different temperatures.

Table 1. Results of the ^{1}H-PSGE and degree aggregation of complex **2** at different temperatures.

T (K)	D_t (10^{-10} m^{2}s^{-1})	r_H^2 (Å)	V_H^2 (Å^3)	V_H^2/V_H^1[a]	n for $[Ag(terpy)]_n^{n+}$
298	11.22	4.68	429.24	1.08	2
280	8.09	5.22	595.27	1.50	3
253	4.83	5.72	782.63	1.98	3.6
233	3.19	5.97	892.53	2.25	4.5
213	1.74	6.96	1412.60	3.57	6.5

[a] V_H^1 =395.62 Å^3 (volume of complex **1** at 298 K)

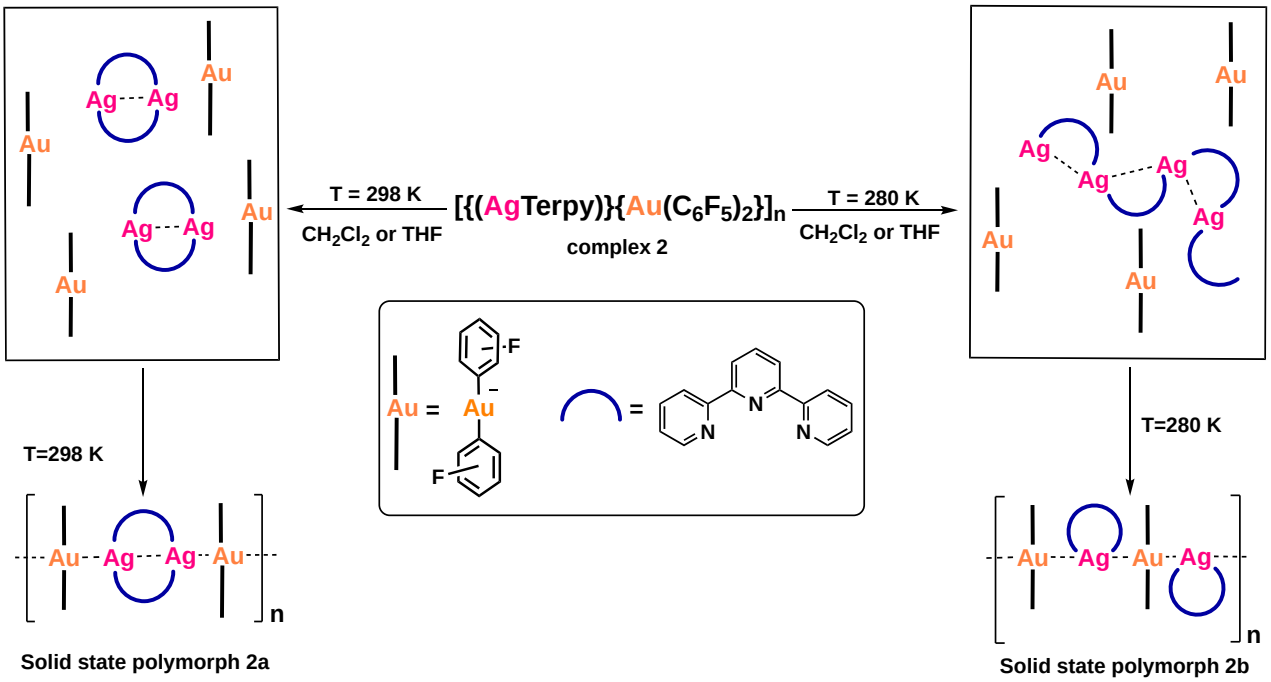

Scheme 3. Temperature-dependent pathways for the synthesis of polymorphs **2a** and **2b**.

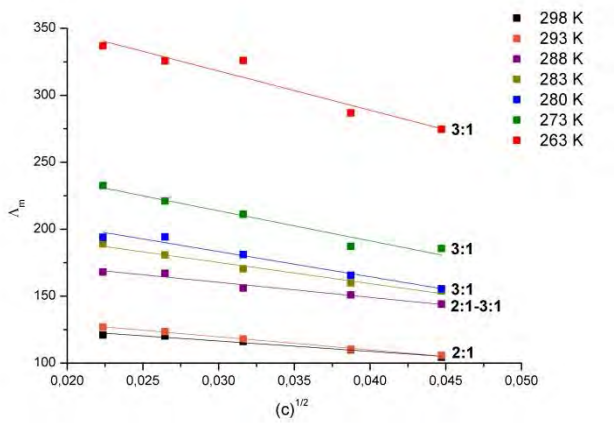

Fig. 5. Graphical representation of the conductivity in solution at different temperatures for complex **2** *vs* the square root of the concentration $(C)^{1/2}$ and linear fit following an Onsager Law model.

Molar conductivity studies at different temperatures

In order to support the PGSE-NMR results, we also carried out a study of the molar conductivity of complex **2** in solution at different temperatures. The study was carried out between 298 and 263 K in acetonitrile (see ESI). Thus, following the Onsager law, the representation of the molar conductivity *vs* the square root of the molar concentration displays a linear behaviour that corresponds to the following equation:

$$\Lambda_m = \Lambda_o - A\sqrt{c}$$

where Λ_m is the molar conductivity, Λ_o is the molar conductivity at infinite dilution, c is the concentration, and the slope A is a coefficient that depends on the nature of the electrolyte, the temperature and the solvent.

Taking into account the previously reported values for A in acetonitrile[23] and the temperature correction to the obtained conductivity values, we have obtained the types of electrolytes formed in solution at different temperatures (see Figure 5 and ESI).

As can be seen, the calculated values clearly match the proposed molecular arrangements in the 298-263 K range. At 298 K the molar conductivity values obtained at different concentrations gives rise to a linear fit with a slope A of 773.9, which is in agreement with the existence of a 1:2 electrolyte

View Article Online
DOI: 10.1039/C9DT00751B
ARTICLE

formed by free $[Au(C_6F_5)_2]^-$ anions and a dinuclear $[Ag(terpy)]_2^{2+}$ cation (see ESI for details). Upon temperature decrease, a clear tendency to the formation of 1:3 electrolytes between 298 and 283 K is observed, with a slope of 1879.0 at 280 K, which corresponds to a 1:3 electrolyte formed by free $[Au(C_6F_5)_2]^-$ and tricationic $[Ag(terpy)]_3^{3+}$ units, in accordance with the PGSE-NMR results.

Thus, in addition to the confirmation of the aggregation process in solution, we can also confirm the role of the aurate(I) anions in solution as a simple counterpart that does not participate of the aggregations process.

Conclusions

We have reported a controlled self-assembly approach for the synthesis of Au(I)-Ag(I) heterometallic complexes displaying different intermetallic interactions sequences by controlling the crystallisation temperature. Among all the factors studied, the only parameter responsible for a different intermetallic ordering is the temperature. The study in solution through NMR techniques and molar conductivity allows us to propose the existence of dimeric $[Ag(terpy)]_2^{2+}$ fragments at 298 K that evolves into oligomeric $[Ag(terpy)]_3^{3+}$ species at lower temperatures, and that this change would be caused by the different crystallisation processes that would take place at different temperatures, leading to distinct polymorphs. Moreover, the crystal structure study also confirms the non-dependence of the metallic arrangement on the solvent.

Acknowledgements

The authors gratefully acknowledge the D.G.I. MINECO/FEDER (project numbers CTQ2016-75816-C2-1-P and CTQ2016-75816-C2-2-P (AEI/FEDER, UE)) and DGA-FSE (E707_17R) for financial support. M. Gil also acknowledges MINECO for a FPI grant.

Notes and references

[a] *Departamento de Química, Universidad de La Rioja, Centro de Investigación en Síntesis Química (CISQ). Complejo Científico-Tecnológico, 26004-Logroño, (Spain). Tel: +34 941299644 E-mail: josemaria.lopez@unirioja.es*

b Departamento de Química Inorgánica, Instituto de Síntesis Química y Catálisis Homogénea (ISQCH), CSIC-Universidad de Zaragoza, E-50009 Zaragoza, Spain. E-mail: gimeno@unizar.es

† Electronic Supplementary Information (ESI) available. CCDC 1813171-1813172. Experimental details. See DOI: 10.1039/b000000x/

1 V. Wing-Wah Yam, V. Ka-Man Au and S. Yu-Lut Leung, *Chem. Rev.*, 2015, **115**, 7589−7728.

2 Q.-M.Wang, Y.-A. Lee, O. Crespo, J. Deaton, C. Tang, H. J. Gysling, M. C. Gimeno, C. Larraz, M. D. Villacampa, A. Laguna and R. Eisenberg, J. *Am. Chem. Soc.*, 2004, **126**, 9488−9489.

3 O. Crespo, M. C. Gimeno, A. Laguna, F. Lahoz and C. Larraz, *Inorg. Chem.*, 2011, **50**, 9533−9544.

4 I. O. Koshevoy, A. J. Karttunen, S. P. Tunik, M. Haukka, S. I. Selivanov, A. S. Melnikov, P. Y. Serdobintsev and T. A. Pakkanen, *Organometallics*, 2009, **28**, 1369−1376.

5 I. O. Koshevoy, A. J. Karttunen, M. Haukka, P.-T. Chou, S. P. Tunik and T. A. Pakkanen, *Chem. Commun*., 2009, 2860−2962.

6 I. O. Koshevoy, A. J. Karttunen, J. R. Shakirova, A. S. Melnikov, M. Haukka, S. P. Tunik and T. A. Pakkanen, *Angew. Chem., Int. Ed*., 2010, **49**, 8864−8866.

7 V. J. Catalano, M. A. Malwitz and A. O. Etogo, *Inorg. Chem*., 2004, **43**, 5714−5724.

8 V. J. Catalano and A. L. Moore, *Inorg. Chem*., 2005, **44**, 6558−6566.

9 E. J. Fernández, M. C. Gimeno, A. Laguna, J. M. López-de-Luzuriaga, M. Monge, P. Pyykkö and D. Sundholm, *J. Am. Chem. Soc*. 2000, **122**, 7287−7293.

10 E. J. Fernández, J. M. López-de-Luzuriaga, M. Monge, M. E. Olmos, R. C. Puelles, A. Laguna, A. Mohamed and J. P. Fackler, *Inorg. Chem*., 2008, **47**, 8069−8076.

11 A. Laguna, T. Lasanta, J. M. López-de-Luzuriaga, M. E. Olmos, M. Monge and P. Naumov, *J. Am. Chem. Soc*., 2010, **132**, 456−457.

12 T. Lasanta, M. E. Olmos, A. Laguna, J. M. López-de-Luzuriaga and P. Naumov, *J. Am. Chem. Soc*., 2011, **133**, 16358–16361.

13 A. A. Mohamed, R. Galassi, F. Papa, A. Burini and J. P. Fackler, Jr., *Inorg. Chem*., 2006, **45**, 7770–7776.

14 Y. Chen, G. Cheng, K. Li, D. P. Shelar, W. Lu and C.-M. Che, *Chem. Sci*., 2014, **5**, 1348−1353.

15 R. Donamaría, M. C. Gimeno,V. Lippolis, J. M. López-de-Luzuriaga, M. Monge and M. E. Olmos, *Inorg. Chem*., 2016, **55**, 11299−11310.

16 M. Gil-Moles, M. C. Gimeno, J. M. López-de-Luzuriaga, M. Monge, M. E. Olmos and D. Pascual, *Inorg. Chem*. 2017, **56**, 9281−9290.

17 (a) E. J. Fernández, A. Laguna, J. M. López-de-Luzuriaga, M. E. Olmos and R. C. Puelles, *Z. Naturforsch*. 2009, **64b**, 1500−1512. (b) E. J. Fernández, A. Laguna, J. M. López-de-Luzuriaga, M. Monge, M. Montiel, M. E. Olmos and M. Rodríguez-Castillo, *Organometallics*, 2006, **25**, 3639−3646. c) J. X. Chen, W. H. Zhang, X. Y. Tang, Z. G. Ren, H. X. Li, Y. Zhang and J. P. Lang, *Inorg. Chem*., 2006, **45**, 7671−7680.

18 J. M. López-de-Luzuriaga, M. Monge, M. E. Olmos, J. Quintana and M. Rodríguez-Castillo, *Dalton Trans*., 2018, **47**, 3231-3238.

19 S. Blomeyer, M. Linnemannstöns, J. H. Nissen, J. Paulus, B. Neumann, H. G. Stammler, N. W. Mitzel, *Angew. Chem., Int. Ed.* 2017, **56**, 13259-13263.

20 E. J. Fernández, A. Laguna, J. M. López-de-Luzuriaga, M. Monge, P. Pyykkö, N. Runerberg, *Eur. J. Inorg. Chem*. 2002, 750-753.

21 V. V. Sivchik, E. V. Grachova, A. S. Melnikov, S. N. Smirnov, A. Y. Ivanov, P. Hirva, S. P. Tunik and I. O. Koshevoy, *Inorg. Chem*., 2016, **55**, 3351−3363.

22 M. J. Hannon, C. L. Painting, E. A. Plummer, L. J. Childs and N. W. Alcock, *Chem. Eur. J*., 2002, **8**, 2225-2238.

23 L. Dutta, D. W. Meek and D. H. Busch, *Inorg. Chem*., 1970, **9**, 1215-1226.

Graphical abstract

Two polymorphs of complex $[\{AuR_2\}Ag(terpy)]_n$ have been obtained through a temperature-controlled approach. These polymorphs display distinct Au-Ag intermetallic arrangements, which are interconvertible through recrystallisation at the appropriate temperature.